Two-Dimensional Space-Charge-Limited Emission: Beam-Edge Characteristics and Applications

R. J. Umstattd and J. W. Luginsland

Air Force Research Laboratory, Directed Energy Directorate, Kirtland Air Force Base, New Mexico 87117

(Received 26 March 2001; published 17 September 2001)

There is, at present, no analytic solution that extends Child-Langmuir space-charge-limited emission beyond 1D. Herein, we investigate the characteristics of planar diode electron emission in 2D space with the emphasis on the transition region between the beam and vacuum. Current density above that predicted by Child-Langmuir is observed near the beam edges in a 2D finite element, electrostatic ray-tracing code. The properties of these increased current density "wings" are examined and then discussed in terms of their applications to cathodes which have large reservoirs of free electrons.

DOI: 10.1103/PhysRevLett.87.145002 PACS numbers: 52.59.Mv

I. Introduction.—The lack of an analytic solution to two- and three-dimensional space-charge-limited emission certainly has not curtailed experimental work in the field. Electron (and ion) beam generation has been done for many years using diodes with two- and three-dimensional features (e.g., Pierce focusing electrodes, hollow anodes, shadow grids, etc. [1,2]). Simulation tools have proven invaluable in advancing the effectiveness of these structures, yet confidence in using such design tools for extremely complex geometries is limited due to the lack of a fundamental analytic description of the problem of multidimensional electrostatic space-charge-limited emission. To use such a design tool here with some level of confidence, we choose to investigate a very simple case of 2D planar space-charge-limited emission. While both the vacuum region and the beam region solutions are well known [3], there is not yet a complete description of the transition region in which these two solutions meet (though recent progress has been made in numerically solving the 2D problem for application in particle-in-cell codes [4]). In an electrostatic ray-tracing code, the standard practice for simulating space-charge-limited emission is to increase current flow in the diode until the electric field at the cathode surface is driven to zero (at which point any increase in emission would be reflected back to the cathode due to the space-charge field of the previously emitted electrons). Such a method is capable of providing highly accurate predictions of physical diode performance even for relatively complicated geometries as is evidenced by the many successful commercial diode designs completed since the advent of numerical simulation tools. Nevertheless, a more complete understanding of 2D emission can improve the diode design process by providing deeper insight into the potential effects of diode geometry. Analytic descriptions of 2D beam *transport* of a given current density profile are available [5] as are investigations into the effects on emission of 2D geometrical features on a cathode surface [6], but the seemingly simple problem of 2D planar space-charge-limited emission remains unsolved.

The simulations performed herein give rise to rules-of-thumb for the nonuniformity of emission that can be expected due to 2D effects. We describe the enhanced (above the Child-Langmuir limit) current density flowing near the edge of the beam and its dependence on applied magnetic field, applied voltage, and diode geometry. We then propose a plausible explanation for this behavior and provide a prescription for controlling in a physical diode the various 2D effects seen here in simulation. These effects play a pivotal role in the development of a complete description of multidimensional space-charge-limited emission.

II. Simulations and results.—The simulations presented here are performed using a 2D finite element, electrostatic ray-tracing code, Trak [7]. A simple planar geometry is assumed (see Fig. 1); the baseline simulation is performed in a Cartesian space with the anode and cathode plates being 10 cm wide (x axis), infinitely long (z axis), and separated by a 1 cm gap (y axis). A 1 kV potential difference is applied across the gap with the cathode being held at zero. A confining magnetic field (0.5 T) is applied along the y axis to simplify electron motion and maintain a sharp transition between the beam and vacuum regions. Space-charge-limited electron emission is allowed only from the central 4 cm region of the cathode surface. We focus on the transition region between space-charge-limited flow and vacuum. Variations on this baseline simulation are then executed and examined relative to the baseline results.

Figure 2 shows the current density emitted at the cathode surface (normalized to the analytic 1D Child-Langmuir value) as a function of position along the cathode (normalized to A-K gap distance) for a sampling of emission strip

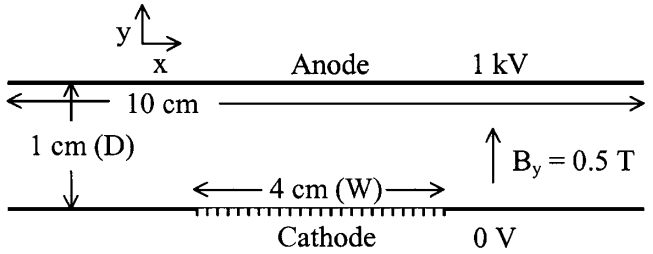

FIG. 1. Geometry and relevant parameters for the baseline 2D emission simulation.

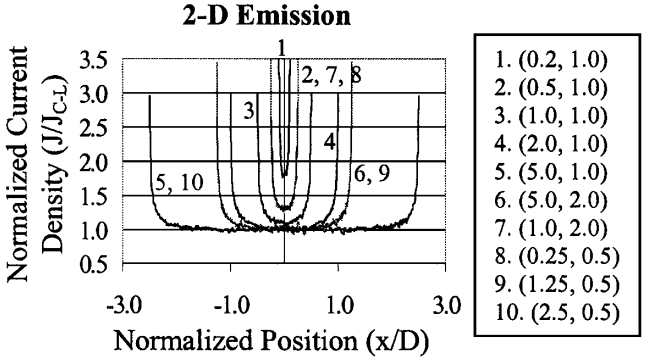

FIG. 2. Simulated normalized current density emitted at cathode versus position (normalized to gap distance) for a variety of emission strip widths (W) and gap distances (D) in cm; each trace is labeled with its corresponding (W, D) value.

widths (W) and gap distances (D). At the beam edge of a flat cathode, there exists no space charge just outside the beam in order to help drive the normal electric field at the last emission point to zero; thus, we posit that extra space charge is emitted (above the 1D Child-Langmuir limit) in order to help drive this local field down. From the scans it is apparent that these high current density "wings" at the beam edge scale with the emission strip width divided by gap distance, W/D (i.e., scans with the same W/D value overlay on the graph). In addition, as the emission strip narrows ($W/D \leq 1$), even the current density at the center of the beam begins to rise above the analytic 1D predicted value. (Such W/D scaling was previously seen by Luginsland *et al.* [8] when simulating *uniform* current density transported in a comparable 2D geometry; similar wing structure was recently described in the numerical solution performed by Watrous *et al.* [4].) Emitted current density wing structure is independent of applied magnetic field, B_y, for tested values of 0, 0.05, 0.1, 0.5, and 0.8 T. Normalized wing structure is also independent of applied anode voltage for values of 10 V, 1 kV, and 100 kV (where current density is normalized by $V^{3/2}$). As the simulation resolution is scanned, the normalized peak current density at the wing tip varies (between $\sim$2.5–3.5), but the remaining shape of the wing is invariant, corresponding to a total current variation of less than 0.5%.

To further pursue the geometry dependence of the wing structure, we examine the effect of having a stepped anode such that the *A-K* gap distance gradually changes from 1 to 0.5 cm, as shown in Fig. 3. Figure 4 is an overlay

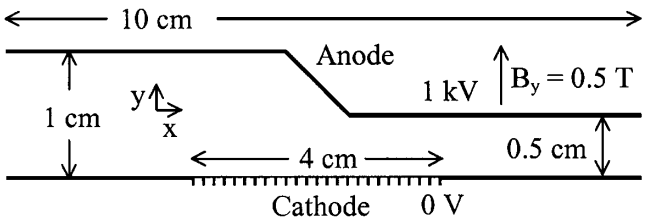

FIG. 3. Geometry and relevant parameters for the stepped anode 2D emission simulation.

of the emitted current density (normalized to a 1D Child-Langmuir 1 cm gap) and the square of the normalized vacuum electric field E_0 perpendicular to the cathode surface. Also shown for comparison is a normalized "local" perveance of the gap ($\propto 1/D^2$).

For this stepped anode case, the emitted current density closely follows the square of the vacuum electric field (except in the wings at the beam edges) rather than the local perveance; this conformity is merely the result of the space-charge-limited emission boundary condition that requires that enough space charge be present to drive the cathode surface normal electric field to zero. Because the analytic 1D current density is proportional to $V^{3/2}/D^2 = E_0^2/V^{1/2}$, it is expected that the local 2D emitted current density will also follow the square of the local vacuum electric field. The data shows that the concept of *local* perveance cannot accurately describe the emission outside of the 1D-like portions of a cathode surface; while perveance still seems appropriate for describing the *global* emission properties of a diode, the data in Fig. 4 show that it is the *local* vacuum electric field that determines the local fluctuations one can expect to see in the emitted current density.

III. Discussion.—From these simulations, it is apparent that the relevant control knob for modifying these high current density wings is the vacuum electric field at the cathode surface. Very small geometry changes in an otherwise uniform diode region can have a significant impact on the local vacuum electric field and, hence, the emitted current density [9]. As stated previously, there exists no space charge just outside the beam to help drive the cathode normal electric field to zero just inside the beam; thus, extra space charge is emitted (above the 1D Child-Langmuir limit) in order to help drive the field down. One can instead compensate for the "missing" space charge at the beam edge by driving the vacuum electric field at the cathode edge down relative to the vacuum electric field at the

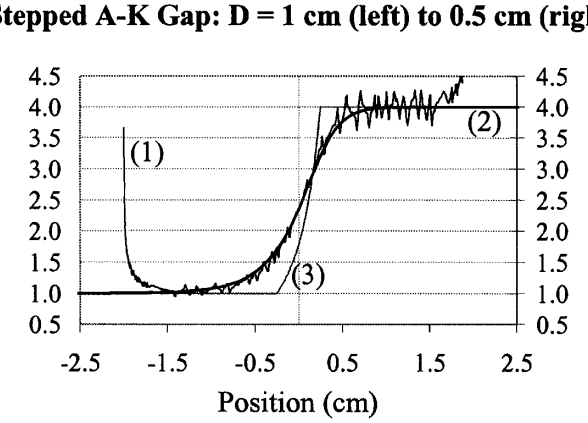

FIG. 4. Overlay of the normalized current density (1), square of the normal component of the vacuum electric field (2), and local perveance (3) for an anode-cathode gap that transitions from 1 to 0.5 cm. The current density in the transition region is seen to closely follow the square of the vacuum electric field rather than the local perveance. (Current density wing on the right side continues off the scale of the graph.)

central portion of the cathode. In a conventional linear microwave tube, a Pierce focusing electrode [10] typically surrounds the cathode in order to provide laminar beam structure; the electrostatic focusing provided by the Pierce electrode geometry negates the space-charge repulsion that attempts to expand the beam. Rather than require a laminar beam, here we will consider the benefits of a more general "focusing" electrode with the sole purpose of lowering the vacuum electric field at the emission edge. Indeed, many planar diode devices have already developed such geometries experimentally. A corona ring or bushing surrounds the typical planar disk cathodes with the primary effect of increasing the uniformity of the electric field across the cathode surface and the secondary effect of reducing the field at the cathode edge relative to the field at the center of the cathode (if the cathode edge is at least slightly recessed below the bushing).

IV. Applications.—The same simulation tool that was used to describe these high current density wings can also be used to investigate geometries for controlling them. First, we will examine how to suppress the enhanced current density for situations where such current densities may damage some portion of the device. Second, we investigate how the presence of the wings may affect our understanding of discrete cathode emission sites working together to provide the total observed current.

As mentioned above, a very slight change in the local vacuum electric field at the cathode edge can have a profound effect on emitted current density. Figure 5 shows a comparison of simulated current density at the beam edge for three cases (with geometry at the edge of the emission surface as shown in the figure). The first is merely the baseline simulation with a perfectly flat, uniform cathode and anode (as in Fig. 1). In the next case, a 0.1-mm-tall Pierce focusing electrode (67.5° angle [10]) has been placed at the beam edge to help suppress the vacuum electric field at the edge; even such a small electrode (1/100th of D) has enough influence to significantly drive down the edge current density. The final case uses a 45°, 0.1-mm-tall focusing electrode. The sharper angle on this electrode has the effect of further reducing the vacuum electric field over the Pierce electrode case with a corresponding reduction in beam-edge current density. Such a drastic reduction in the edge current density comes at the cost of having an enhanced electric field on the focusing electrode structure; the focusing electrode reduces the vacuum electric field at certain locations by increasing the field at other locations (as is the nature of an electrostatic solution).

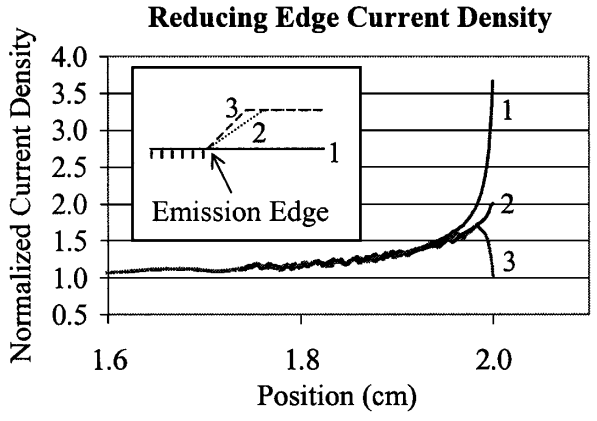

FIG. 5. Comparison of simulated current densities near the beam edge when the beam edge has either no focusing (case 1 of inset—an expanded view of the cathode surface of the standard diode from Fig. 1), a 0.1-mm-tall Pierce electrode (case 2 of inset), or a 0.1-mm-tall 45° electrode (case 3 of inset).

To examine how these increased current density wings might affect total current, we suppress emission from some portion of the cathode in two different fashions and monitor changes in the total current. In the first method, we divide the baseline 4-cm-wide emission region into 40 separate, equal-width subregions. As we systematically decrease the portion of each subregion that is allowed to emit, little effect is seen on the total current emitted until nearly all of the cathode emission area has been turned off. This behavior is shown in the upper trace of Fig. 6. Almost 80% of the full emission area current can be supplied by a mere 20% of emitting cathode area due to the ability of the enhanced current density wings to compensate for the paucity of emission area. In the second method, this effect was further examined by suppressing emission from only a central portion of the cathode. The nonemitting portion was gradually increased in size as the total current was monitored (also shown in Fig. 6). From the figure it is clear that the 2 sets of wings present at the two edges of the nonemitting portion cannot compensate for the nonemitting area nearly as well as the 40 sets of wings available in the discrete patches case. Such an effect has direct relevance to understanding space-charge-limited emission from explosive emission cathodes, plasma cathodes, ferroelectric cathodes, photocathodes, and even thermionic

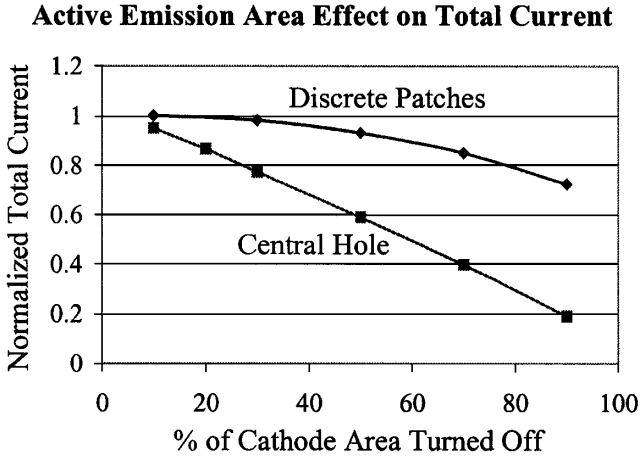

FIG. 6. Reduction of total emitted current due to the reduction of an allowed emission area on a 4-cm-wide cathode strip. The current is normalized to the simulation result for emission from 100% of the cathode area. The cathode is divided into 40 individual sections which are gradually turned off (discrete patches), or a sole nonemitting hole is allowed to expand from the cathode center (central hole).

cathodes (if operating well above the temperature-limited regime). *Many small portions of the emission surface may be completely inactive before a significant change is detected in the observed total current.* In a plasma-based cathode (including explosive or ferroelectric emission) such an effect may be masked due to plasma filling in the gaps between emission sites. Nevertheless, as these cathodes are driven into regimes where the plasma is cooler and less dense, the total current emitted is not expected to change even if the plasma no longer completely fills the gaps between emission sites. This effect must be taken into account when developing an understanding of a plausible death mechanism for such cathodes. If a sole region ceases to emit and then continues to enlarge in area, one would expect to see a nearly linear reduction in the total current. If the emission is instead being provided by numerous microsites, many such sites could be turning off and on multiple times during the life of a given cathode with little or no effect on the observed total current.

Figure 7 is a photograph of a few standard cathode/holder assemblies used at the Air Force Research Lab for cathode evaluation [11]. The emission surfaces are explosive emitters with active regions that combine to occupy only between $\sim 0.5\%-5.0\%$ of the total cathode area (plasma formation most likely helps to fill in any gaps between active regions). Each cathode is surrounded by a metallic bushing ring covered with an insulating layer (to prevent emission from the bushing). Such a geometry has proven to be quite reliable for testing a variety of cathode and anode materials. Because the cathode edge is recessed slightly below the bushing edge (thereby making the bushing function as a focusing electrode), damage patterns on various planar anodes show no enhancement at the beam edge corresponding to the suppression of the high current density wings. Various cathode materials with a variety of active emission areas (but identical bulk area) have all been examined; even though the cathodes differ significantly in their microgeometry, they each provide the same total current. Geometry differences on the cathode surface that are roughly of the same scale or smaller than the diode gap should have little effect on the total current, in large part due to the increased current density available in the wings of the cathode microstructure.

V. Summary.—Current densities well above that predicted by 1D space-charge-limited theory are observed in 2D simulations of basic geometries. The structure of the enhanced current density wing at the beam edge is independent of applied magnetic field and voltage and is a function solely of diode geometry (W/D). The local emitted current density scales with the square of the vacuum electric field rather than with the local perveance. Simulations show that small changes in the local field near the cathode edge can have a significant impact on these high current density wings. In addition, the presence of such wings on a small scale in a micropoint emitter can effectively mask microgeometry differences by providing nearly identical total bulk currents for a variety of cathode microgeometries.

FIG. 7. Photograph of a sampling of cathode types tested at AFRL in identical bushing rings (courtesy of D. A. Shiffler). Top: cesium iodide-coated carbon tufts. Right: metal finger stock on ceramic shutters. Bottom: polymer velvet. Left: cesium iodide-coated carbon fibers.

The authors thank colleagues, D. A. Shiffler, T. A. Spencer, C. S. Brodel, and J. J. Watrous, for their insightful comments during numerous discussions of this topic. This work is supported by the Air Force Office of Scientific Research.

[1] M. Reiser, *Theory and Design of Charged Particle Beams* (Wiley, New York, 1994).
[2] A. S. Gilmour, Jr., *Microwave Tubes* (Artech House, Dedham, MA, 1986).
[3] C. D. Child, Phys. Rev. **32**, 492 (1911); I. Langmuir, *ibid.* **2**, 450 (1913).
[4] J. J. Watrous, J. W. Luginsland, and G. E. Sasser III, Phys. Plasmas **8**, 289 (2001).
[5] P. T. Kirstein, G. S. Kino, and W. E. Waters, *Space Charge Flow* (McGraw-Hill, New York, 1967).
[6] J. M. Finn, T. M. Antonsen, Jr., and W. M. Manheimer, IEEE Trans. Plasma Sci. **16**, 281 (1988).
[7] Simulations were performed using portions of the Tri-Comp suite of finite-element electromagnetic software available from Field Precision, Albuquerque, NM (see http://www.fieldp.com/).
[8] J. W. Luginsland, Y. Y. Lau, and R. M. Gilgenbach, Phys. Rev. Lett. **77**, 4668 (1996).
[9] R. J. Umstattd, D. A. Shiffler, C. A. Baca, K. J. Hendricks, T. A. Spencer, and J. W. Luginsland, Proc. SPIE Int. Soc. Opt. Eng. **4031**, 185 (2000).
[10] J. R. Pierce, *Theory and Design of Electron Beams* (Van Nostrand, New York, 1954), 2nd ed., Chap. 10.
[11] D. A. Shiffler, M. Lacour, K. Golby, M. D. Sena, R. J. Umstattd, J. Luginsland, K. Hendricks, T. Spencer, and A. Gibbs, Proc. SPIE Int. Soc. Opt. Eng. **4031**, 144 (2000).